

Entrance channel dependence and isospin dependence of preequilibrium nucleon emission in intermediate energy heavy ion collisions

Jian-Ye Liu^{a,b,c}, Qiang Zhao^c, Shun-Jin Wang^{a,b,d}, Wei Zuo^{a,b,c}, Wen-Jun Guo^c

^aCCAST (World Laboratory), P. O. Box 8130, Beijing 10080, P. R. China

^bCenter of Theoretical Nuclear Physics, National Laboratory of Heavy Ion Accelerator, Lanzhou 730000, P. R. China

^cInstitute of Modern Physics, Chinese Academy of Sciences, P. O. Box 31, Lanzhou 730000, P. R. China

^dInstitute of Modern Physics, southwest Jiaotong University, Chendu 610031, P. R. China

Abstract

Using isospin dependent quantum molecular dynamical model, the studies of the isospin effect on preequilibrium nucleon emission in heavy ion collisions under different entrance channel conditions show that the ratio of preequilibrium neutron number to proton number depends strongly on symmetry potential, beam energy, and the ratio of neutron to proton of the colliding system, but weakly on isospin dependent in-medium nucleon-nucleon cross sections, impact parameter, Pauli potential, and momentum dependent interaction in the energy region from 45 MeV/u up to 150 MeV/u where the dynamics is dominated by nucleon-nucleon collisions. In addition, the ratio of preequilibrium neutron number to proton number for a neutron-rich colliding system is larger than the initial value of the ratio of the colliding system, but the ratio for a neutron-deficient system is less than the initial value.

PACS number(s): 25.70.Pq, 02.70.Ns, 24.10.Lx

Keywords: isospin effect of preequilibrium nucleon emission, probe to symmetry potential, in-medium nucleon-nucleon cross sections

1 Introduction

During the heavy ion collisions induced by stable or radioactive nuclei with different neutron to proton ratios, thermal and compressed nuclear states with different isospin asymmetries can be created. The properties of these nuclear states and their subsequent fragmentation products depend sensitively on the neutron to proton ratio of the colliding system, the symmetry potential, and the isospin dependence of in-medium nucleon-nucleon (N-N) cross section. Thus, the information on the equation of state (EOS) of isospin asymmetric nuclear matter can be extracted by making a comparison between theoretical calculations and experiment data [1-5] in a wide domain of isospin degree of freedom ranging from symmetric nuclear matter to pure neutron matter. R. Pak and Bao-An Li et al. suggested to extract the information of in-medium N-N cross section by studying the isospin dependences of collective flow and balance energy [6-9]. We also proposed that the information of in-medium N-N cross section can be extracted by studying isospin effects of multifragmentation in heavy ion collisions at some chosen beam energies [10]. Bao-An Li et al. [11] have found that the information of symmetry potential can be extracted by studying the ratio of preequilibrium neutrons to protons in heavy ion collisions at relatively low beam energy ($E \leq 100MeV/u$). However, most of investigations on the ratio of preequilibrium neutrons to protons in heavy ion collisions concentrated at the energies nearby the Fermi energy and made use of the isospin-dependent BUU model.

As is well known that the outcome of heavy ion collisions depends sensitively on entrance channel conditions. In this paper, we shall investigate systematically the entrance channel dependence of the isospin effect on preequilibrium nucleon emission in heavy ion collisions by using the isospin dependent quantum molecular dynamics

[12](IQMD) with momentum dependence interaction (MDI) and Pauli potential. The calculated results show that the ratio of the preequilibrium neutrons to protons depends strongly on the symmetry potential, the initial ratio of neutrons to protons of the colliding system, and the beam energy, but weakly on the isospin dependence of in-medium N-N cross section, the impact parameter, the Pauli potential, and the momentum dependent interaction in the energy region from 45 MeV/u to 150 MeV/u where the dynamics is dominated by N-N collisions. The ratio of preequilibrium neutron number to proton number for the neutron-rich colliding systems is larger than the initial value of the neutron-proton ratio of the colliding systems, but the ratio for neutron-deficient systems is less than the initial value.

2 Theoretical model and its parameters

In order to describe the isospin effects on the dynamical process of heavy ion collisions, quantum molecular dynamics (QMD) [13] should be modified properly: the density dependent mean field should contain the correct isospin-dependent terms, such as symmetry energy and Coulomb potential, the in-medium N-N cross section should be different for neutron-neutron (proton-proton) and neutron-proton collisions, and finally Pauli blocking should be counted by distinguishing neutrons and protons. In addition, in our calculations, Pauli potential and momentum dependent interaction (MDI) are also included in the interaction potential which contains Skyrme, Coulomb, Yukawa, symmetry, Pauli potential and MDI, their formula are as follows

U^{Sky} is the Skyrme potential

$$U^{Sky} = \alpha\left(\frac{\rho}{\rho_0}\right) + \beta\left(\frac{\rho}{\rho_0}\right)^\gamma \quad (1)$$

U^{coul} is the Coulomb potential. The Yukawa potential acting on particle j is given by the expectation value of U^{Yuk} interaction [13]

$$U_j^{Yuk} = t_3 \sum_{i \neq j} \frac{e^{L/m^2}}{r_{ij}/2m} \{ e^{-r_{ij}/m} [1 - \Phi(\sqrt{L}/m - r_{ij}/2\sqrt{L})] - e^{r_{ij}/m} [1 - \Phi(\sqrt{L}/m + r_{ij}/2\sqrt{L})] \} \quad (2)$$

where Φ is the error function. U^{MDI} is the momentum dependent interaction

$$U^{MDI} = t_4 \ln^2 [t_5 (\vec{p}_1 - \vec{p}_2)^2 + 1] \frac{\rho}{\rho_0} \quad (3)$$

U^{Pauli} is the Pauli potential

$$U^{Pauli} = V_p \left(\frac{\hbar}{p_0 q_0} \right)^3 \exp \left(- \frac{(\vec{r}_i - \vec{r}_j)^2}{2q_0^2} - \frac{(\vec{p}_i - \vec{p}_j)^2}{2p_0^2} \right) \delta_{p_i p_j} \quad (4)$$

$$\delta_{p_i p_j} = \begin{cases} 1 & \text{for neutron-neutron or proton-proton} \\ 0 & \text{for neutron-proton} \end{cases}$$

which is used to describe Pauli blocking at the mean field level [14]. According to our experience, the mean field containing Pauli potential can describe the structure effect of fragmentation in the process of heavy ion collisions [15]. U^{sym} is the symmetry potential

$$U^{sym} = C \frac{\rho_n - \rho_p}{\rho_0} \tau_z \quad (5)$$

$$\tau_z = \begin{cases} 1 & \text{for neutron} \\ -1 & \text{for proton,} \end{cases}$$

where C taking the values of 0 or 32MeV, is the strength of the symmetry potential.

First of all, Skyrme-Hatree-Fock code with parameter set SKM* [19] is employed to get the density distributions and root mean square (RMS) radii for the neutrons and protons of each colliding nucleus studied. For example, in Fig.1 is given the density distributions for the neutron-rich nucleus ^{80}Zn and the neutron-deficient nucleus ^{76}Kr . It is clear seen that there is a tail for the neutron distribution of the neutron-rich

nucleus ^{80}Zn , but the difference between the neutron distribution and the proton distribution of the neutron-deficient nucleus ^{76}Kr is very small. The ground state of each colliding nucleus is then prepared according to the obtained above density distributions in coordinate space and Fermi distribution in momentum space by using Monte-Carlo sample. The parameters of the interaction potentials are given in table 1, where the parameters of Skyrme and MDI are taken from Ref. [20] and those of Pauli potential refer to Ref.[10].

α	β	γ	t_3	m	t_4	t_5	V_p	p_0	q_0
(MeV)	(MeV)		(MeV)	(fm)	(MeV)	(MeV ⁻²)	(MeV)	(MeV/c)	(fm)
-390.1	320.3	1.14	7.5	0.8	1.57	5×10^{-4}	30	400	5.64

Table 1. The parameters of the interaction potentials

The following empirical expression is used for the in-medium N-N cross section [16]

$$\sigma_{NN}^{med} = (1 + \alpha \frac{\rho}{\rho_0}) \sigma_{NN}^{free}, \quad (6)$$

with $\alpha = -0.2$. σ_{NN}^{free} is the experimental free N-N cross section from [17].

The neutron-proton cross section is about 3 times larger than the proton-proton or neutron-neutron cross section below about 500MeV.

In order to check the IQMD code with the above parameters, the multiplicity of intermediate mass fragments N_{imf} for the reactions $^{58}\text{Fe} + ^{58}\text{Fe}$ and $^{58}\text{Ni} + ^{58}\text{Ni}$ at the beam energy $E = 75\text{MeV/u}$ has been calculated by using the IQMD code. The intermediate mass fragments (IMFs) are defined as the fragments with charge numbers greater than 3 and less than 18. The calculated results are compared with the experimental data [18] in the same scaler in Fig. 2 which gives the correlation between the mean value of the intermediate mass fragment multiplicity N_{imf} and the charged particle multiplicity N_c . The solid (open) circles represent the experimental

data for the reaction $^{58}\text{Ni} + ^{58}\text{Ni}$ ($^{58}\text{Fe} + ^{58}\text{Fe}$) at $E = 75\text{MeV/u}$ and the solid line (dot line) denotes the IQMD results for $^{58}\text{Ni} + ^{58}\text{Ni}$ ($^{58}\text{Fe} + ^{58}\text{Fe}$). It is clear that the present IQMD predictions are in a satisfactory agreement with general features of the experimental data.

3 Results and Discussions

As is well known that the isospin effects on the reaction mechanism and the reaction products in heavy ion collisions depend sensitively on the entrance channel conditions, such as the neutron-proton ratio, the total mass of the colliding system, the beam energy, and the impact parameter. In this paper, the entrance channel dependence of preequilibrium nucleon emission for the two neutron-rich systems $^{76}\text{Zn} + ^{76}\text{Zn}$ ($\frac{N}{Z} = 1.53$) and $^{80}\text{Zn} + ^{80}\text{Zn}$ ($\frac{N}{Z} = 1.67$), and for the neutron-deficient system $^{76}\text{Kr} + ^{76}\text{Kr}$ ($\frac{N}{Z} = 1.11$) are studied by using IQMD in the beam energy region from 45 MeV/u to 150 MeV/u.

Fig. 3 shows the time evolutions of the ratio of preequilibrium neutrons to protons $\frac{N_n}{N_p}$ for the three colliding systems $^{80}\text{Zn} + ^{80}\text{Zn}$ (top window), $^{76}\text{Zn} + ^{76}\text{Zn}$ (middle window), and $^{76}\text{Kr} + ^{76}\text{Kr}$ (bottom window) at the beam energies $E=45\text{MeV/u}$ (left column), 120MeV/u (middle column), and 150MeV/u (right column), and at the impact parameter $b=1.0$ fm for the following three cases:

- 1) $U^{sym} + \sigma^{Iso}$ (solid line), indicating symmetry potential and isospin dependent in-medium N-N cross section;
- 2) $U^{sym} + \sigma^{Noiso}$ (dash line), indicating symmetry potential and isospin independent in-medium N-N cross section;
- 3) $C=0$ MeV+ σ^{Iso} (dot line), indicating isospin dependent in-medium N-N cross sections without symmetry potential.

σ^{Iso} and σ^{Noiso} denote the isospin dependence N-N cross section and isospin independence N-N cross section, respectively. In the case of σ^{Iso} , the neutron-proton cross section σ_{np}^{Iso} is about three times larger than the neutron-neutron cross section σ_{nn}^{Iso} below about 500MeV. But in the case of σ^{Noiso} , $\sigma_{np}^{Noiso} = \sigma_{nn}^{Noiso} = \sigma_{nn}^{Iso}$ [17].

The preequilibrium nucleon emission is defined as to include all neutrons and protons emitted before the colliding system has reached the thermal equilibrium. From the time evolution of the nucleon quadrupole momentum distribution Q_{zz} (right window) in Fig. 4 and those of neutron number (middle window) and proton number (right windows) in Fig. 5, we see that the colliding systems reach thermal equilibrium and the single particle emission approaches a constant value before 200fm/c and $\frac{N_n}{N_p}$ reaches about constant value at about 100fm/c. The nucleon is considered to be free if it is not correlated with other nucleons within a spatial distance of $\Delta r = 3\text{fm}$ and a momentum distance of $\Delta p = 300\text{MeV}/c$ as in [1]. In addition, in the early stage of the reaction, the neutron excess is seen to fluctuate due to violent N-N collisions. So the colliding duration in the figures is from 60 fm/c to 200 fm/c.

From Fig. 3 we can see that $\frac{N_n}{N_p}$ depends strongly on the symmetry potential, but weakly on the isospin-dependent in-medium N-N cross section in the energy region from 45MeV/u to 150MeV/u. At relatively large beam energy ($E > 100\text{MeV}/u$), the isospin effects of the N-N cross sections on the dissipation-fluctuation and fragmentation process are obvious from Fig. 4, where is plotted the time evolution of the intermediate mass fragment multiplicity N_{imf} (left window) and the nucleon quadrupole momentum distribution Q_{zz} (right window) for the system $^{80}\text{Zn} + ^{80}\text{Zn}$ at $E=120\text{ MeV}/u$ and $b=1.0\text{fm}$ in the three cases. From Fig. 3 one can also see that the influence of the beam energy on the ratio of preequilibrium neutrons to protons is salient.

The left window of Fig. 5 shows the time evolution of $\frac{N_n}{N_p}$ for the three collision

systems at $E=100$ MeV/u and $b=1.0$ fm in the case of ($U^{sym} + \sigma^{Iso}$). $\frac{N_n}{N_p}$ for the neutron-rich systems $^{80}Zn + ^{80}Zn$ (dot-dash line) and $^{76}Zn + ^{76}Zn$ (dot line) are 1.83 and 1.62 which are larger than the initial values of the colliding systems: $(\frac{N_t+N_p}{Z_t+Z_p}) = 1.67$ and 1.53 , respectively. Here N_p, N_t, Z_p and Z_t are the neutron number and proton number for the projectile and target, respectively. Because the symmetry potential tends to make more neutrons than protons to be unbound (compare the time evolutions of preequilibrium neutron number and proton number in the middle window and right window in Fig. 5), one thus expects that a stronger symmetry potential leads to a larger ratio of neutrons to protons.

From the left window of Fig. 5 one can also see that $\frac{N_n}{N_p}$ for the neutron-deficient colliding system $^{76}Kr + ^{76}Kr$ (solid line) is quite different from that for the neutron-rich colliding system. For instance, its ratio of preequilibrium neutron number to proton number is 1.06 being less than its initial value of $(\frac{N_t+N_p}{Z_t+Z_p})$ of 1.11. The mechanism about that can be explained as follows. On the one hand, the symmetry potential tends to make more neutrons than protons to be unbound; on the other hand, the Coulomb interaction tends to make more protons than neutrons to be unbound (see solid lines in the middle window and the right window of Fig. 5). The final result depends on the competition between the two factors. For the neutron-rich colliding systems, the effect of symmetry potential is stronger than that of Coulomb interaction, more neutrons will be emitted than protons and $\frac{N_n}{N_p}$ will be larger than its initial value. On the contrary, for the neutron-deficient colliding systems, Coulomb effect is stronger than that of the symmetry potential, less neutrons will be emitted than protons and $\frac{N_n}{N_p}$ will be less than its initial value. Nevertheless, for both neutron-rich and neutron-deficient colliding systems, the ratio of preequilibrium neutron number to proton number depends always strongly on the symmetry potential and weakly on the

in-medium isospin dependent N-N cross section in the energy region from 45 MeV/u to 150 MeV/u.

Figure 6(a) shows the time evolutions of $\frac{N_n}{N_p}$ for the system $^{80}\text{Zn} + ^{80}\text{Zn}$ at $E=150$ MeV/u and $b=1.0$ fm in three cases:

- 1) indicating Pauli and momentum-dependent interaction (denoted by “p, m” and solid line);
- 2) indicating Pauli potential without momentum-dependence interaction (denoted by “p, nom” and dot line);
- 3) without both of them (denoted by “nop, nom” and dash line).

It is clear to see that the effects of Pauli potential and the momentum dependent interaction on the $\frac{N_n}{N_p}$ are very poor.

In Figs. 6(b, c, d) are shown the time evolutions of $\frac{N_n}{N_p}$, N_n , and N_p for the reaction $^{80}\text{Zn} + ^{80}\text{Zn}$ at $E=150$ MeV/u, $b=1.0$ fm (solid line), and $b=5.0$ fm (dot line). Though the numbers of preequilibrium neutron and proton decrease as increasing impact parameter b (see Figs. 5(c, d)), the ratio $\frac{N_n}{N_p}$ only slightly increases with increasing impact parameter, which is in agreement with the result of Bao-An Li et al. [1] (see Fig. 5(b)).

Fig. 7 indicates the impact parameter averaged kinetic energy spectra ($b=0.0-3.0$ fm) of preequilibrium neutron-proton ratio for the system $^{76}\text{Zn} + ^{76}\text{Zn}$ at $E=100$ MeV/u and in the three cases as the same as in Fig. 3. It is clear to see that the conclusion about that $\frac{N_n}{N_p}$ depends sensitively on the symmetry potential and weakly on the in-medium isospin dependence N-N cross section has remained the same .

4 Conclusion

In summary, the entrance channel dependence of the isospin effect of the preequilibrium nucleon emission for the neutron-rich colliding systems and neutron-deficient colliding

systems have been studied systematically by using IQMD in a wide region of beam energies. The calculated results show that the ratio of preequilibrium neutron number to proton number depends strongly on the symmetry potential, the neutron-proton ratio of the colliding system, and the beam energy, but weakly on the isospin dependence of the in-medium N-N cross section, in the energy region from 45MeV/u to 150 MeV/u. The Pauli potential, the momentum dependent interaction, and the impact parameter also have a sizable effect on the preequilibrium nucleon emission, but the effects of the three factors on neutron emission are nearly the same as on proton emission, so the preequilibrium neutron-proton ratio depends slightly on the impact parameter, MDI and Pauli potential. The ratio of preequilibrium neutron number to proton number for the neutron-rich colliding system is larger than the initial value of the system, but that for the neutron-deficient colliding system is less than its initial value. The present investigation also supports the suggestion by Bao-An Li et al. using BUU calculations [1] that the ratio of preequilibrium neutron number to proton number in HIC can be used as a probe to extract the information on the symmetry potential. However our investigation has extended the energy region of the applicability of this suggestion from the beam energy $E < 100$ MeV/u to relatively higher beam energy up to $E = 150$ MeV/u.

Acknowledgment

This work was supported in part by the “100 person project” of the Chinese Academy of Sciences, ”973 project” under Grant number G2000077400, the National Natural Science Foundation of China under Grants No. 19775057 and No. 19775020, No. 19847002, No. 19775052 and KJ951-A1-410, by the Foundation of the Chinese Academy of Sciences.

References

- [1] B. A. Li, C. M. Ko and W. Bauer , *Inter. Jour. Mod. Phys.* **E7**(1998)147-229.
- [2] L. B. Yang, E. Norbeck and W. A. Friedman et al., *Phys. Rev.* **C60**(1999)041602.
- [3] B. A. Li and C. M. Ko, *Phys. Rev.* **C57**(1998) 2065.
- [4] B. A. Li and S. J. Yennello, *Phys. Rev.* **C52**(1995)1746.
- [5] M. S. Hussein, R. A. Rego and C. A. Bertulani, *Phys. Rep.* **201**(1991)279.
- [6] B. A. Li, Z. Z. Ren, C. M. Ko and S. J. Yennello, *Phys. Rev. Lett.* **76**(1996)4492.
- [7] R. Pak, W. Benenson and O. Bjarki et al., *Phys. Rev. Lett.* **78**(1997)1022.
- [8] R. Pak, B. A. Li and W. Benenson et al., *Phys. Rev. Lett.* **78**(1997)1026.
- [9] Y. M. Zhong, B. A. Li and C. M. Ko, *Phys. Rev. Lett.* **83**(1999)2534-2536.
- [10] Qiang Zhao, Wen-Jun Guo, Jian-Ye Liu and Wei Zuo, *High Energy Physics and Nuclear Physics* to be published.
- [11] B. Jouault et al., *Preprint SUBATECH-95-11*.
- [12] Lie-Wei Chen, Feng-Show Zhang and Ge-Ming Jin, *Phys. Rev.* **C58**(1998)2283; Feng-Show Zhang, Lie-Wei Chen, Zhao-Yu Ming and Zhi-Yuan Zhu, *Phys. Rev.* **C60**(1999)064604-1.
- [13] J. Aichelin, G. Peilert and A. Bohnet, A.Rosenhauer, H.Stöcker and W. Greiner, *Phys. Rev.* **C37**(1988)2451.
- [14] C. Dorso, S. Duarte and J. Randrup, *Phys. Lett* **B188**(1987)287.
- [15] Liu Hang and Liu Jian Ye, *Z. Phys.* **A345**(1996)311.
- [16] D. klakow, G. Welke and W. Bauer, *Phys. Rev.***C36**(1993)1982.
- [17] K. Chen, Z. Fraenkel and G. Friedlander et al., *Phys. Rev.***166**(1968)949.
- [18] M. L. Miller, O. Bjarki and D. J. Magestro et al., *Phys.Rev.Lett.***82**(1999)1399.

- [19] P. G. Reinhard, in Computational Nuclear Physics 1, edited by K. Langanke, J. A. Maruhn, and S. E. Koonin, Germany, Springer-Verlag, 1991, P. 28-50.
- [20] J. Aichelin, A. Rosenhauer, G. Peilert, H. Stöcker and W. Greiner., *Phys. Rev. Lett* **Vol.58**(1987)1402-1419.

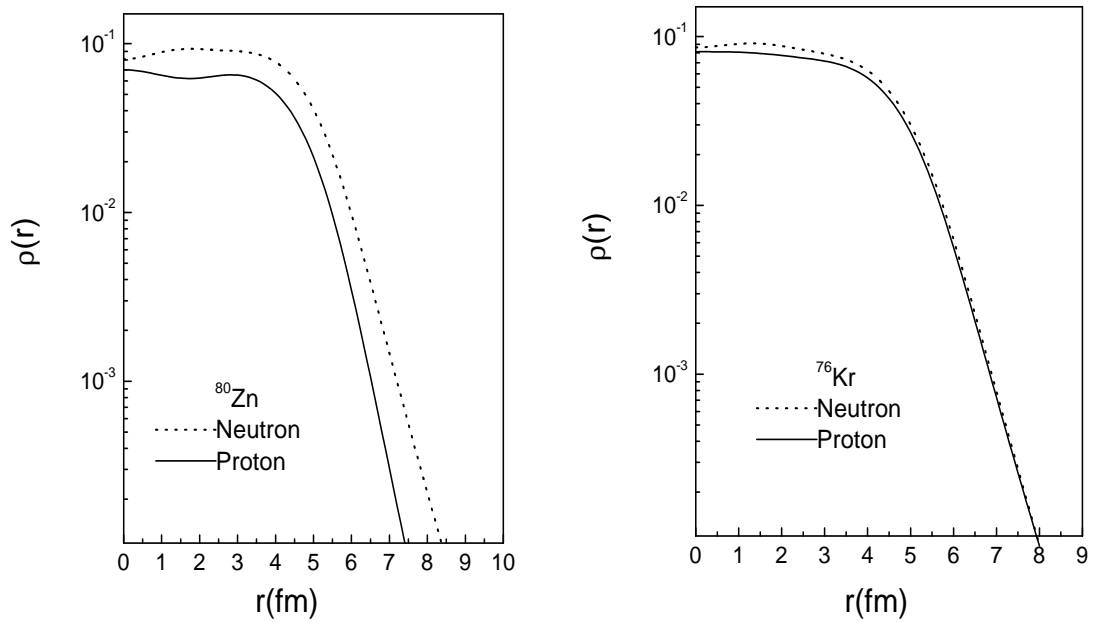


Figure 1: The density distribution of ^{80}Zn (left window) and that of ^{76}Kr (right window), solid lines indicates the protons distribution and dot lines for neutrons distribution.

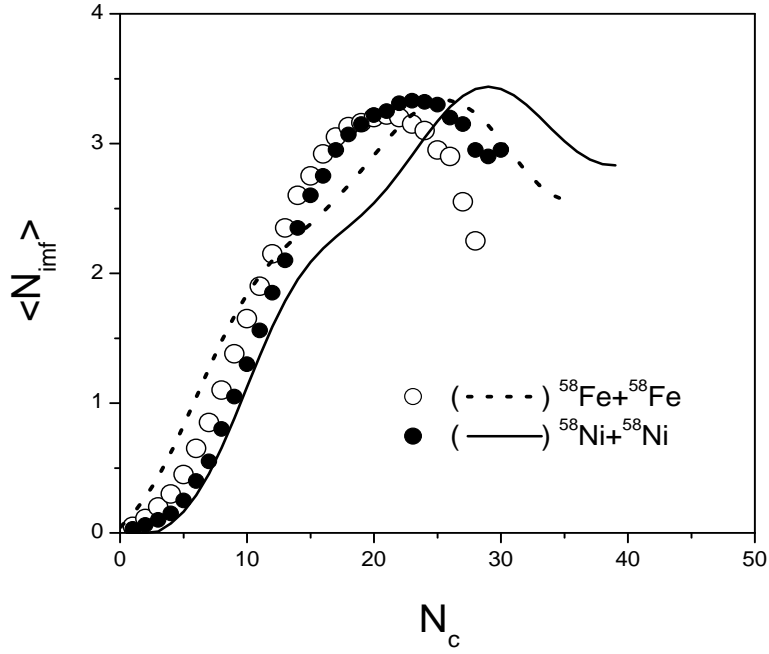


Figure 2: The correlation between the mean intermediate mass fragment multiplicity N_{imf} and the charged particle multiplicity N_c . Filled (unfilled) circles represent the experimental data [18] for the reactions $^{58}\text{Ni} + ^{58}\text{Ni}$ ($^{58}\text{Fe} + ^{58}\text{Fe}$) at $E=75$ MeV/u and the solid line (dot line) indicates the IQMD results for $^{58}\text{Ni} + ^{58}\text{Ni}$ ($^{58}\text{Fe} + ^{58}\text{Fe}$). The charge number of N_{imf} is taken from 3 to 18

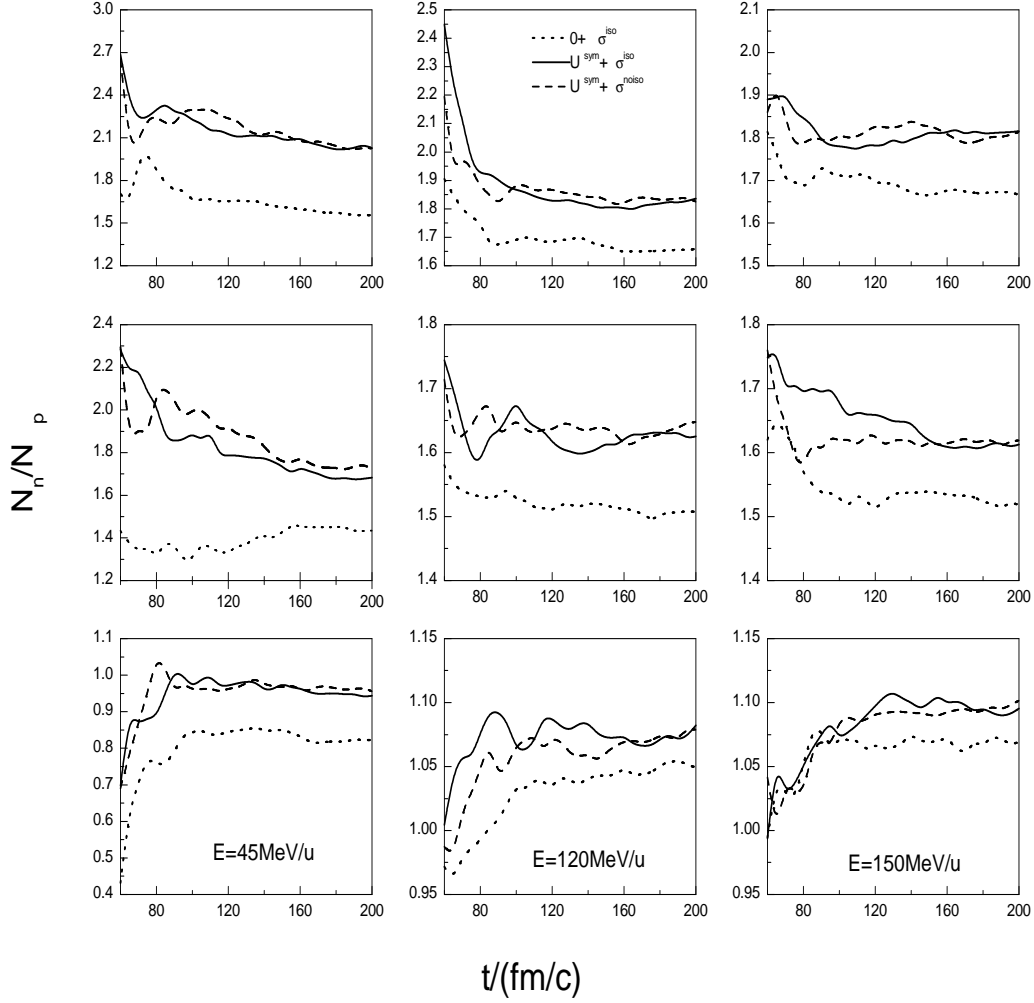


Figure 3: The time evolution of N_n/N_p for the systems $^{80}\text{Zn}+^{80}\text{Zn}$ (top row), $^{76}\text{Zn}+^{76}\text{Zn}$ (middle row), and $^{76}\text{Kr}+^{76}\text{Kr}$ (bottom row) at $E=45\text{MeV/u}$ (left column), $E=120\text{MeV/u}$ (middle column), $E=150\text{MeV/u}$ (right column) and $b=1.0\text{fm}$. Solid lines for $U^{sym} + \sigma^{iso}$, dash lines for $U^{sym} + \sigma^{noiso}$, and dot lines for $0 + \sigma^{iso}$.

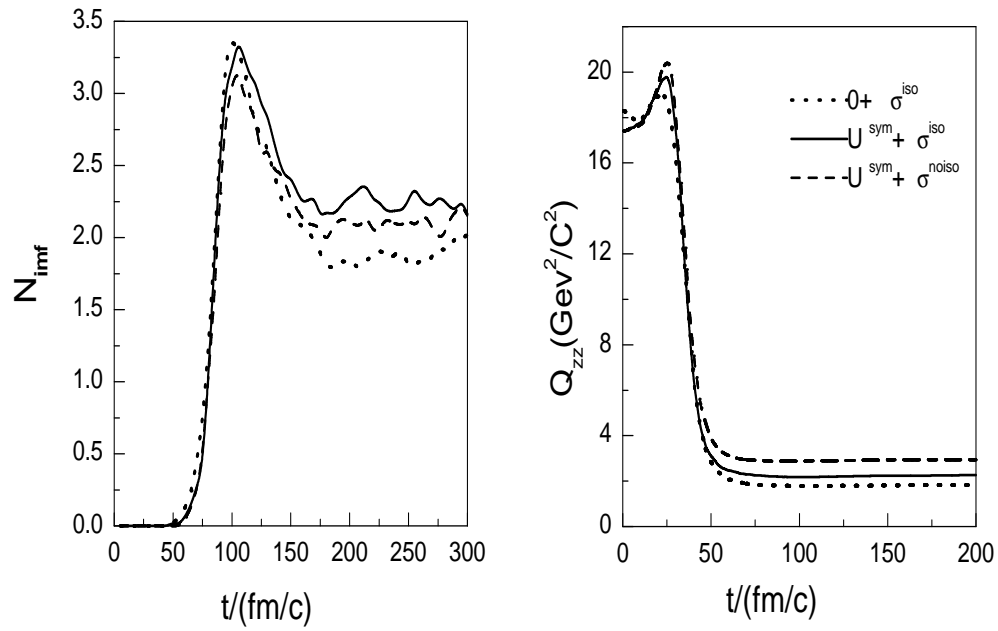


Figure 4: The time evolution of N_{imf} (left window) and Q_{zz} (right window) for the system $^{80}\text{Zn}+^{80}\text{Zn}$ at $E=120\text{MeV}/u$ and $b=1.0\text{fm}$. Solid lines for $U^{sym} + \sigma^{iso}$, dash lines for $U^{sym} + \sigma^{noiso}$, and dot lines for $0 + \sigma^{iso}$.

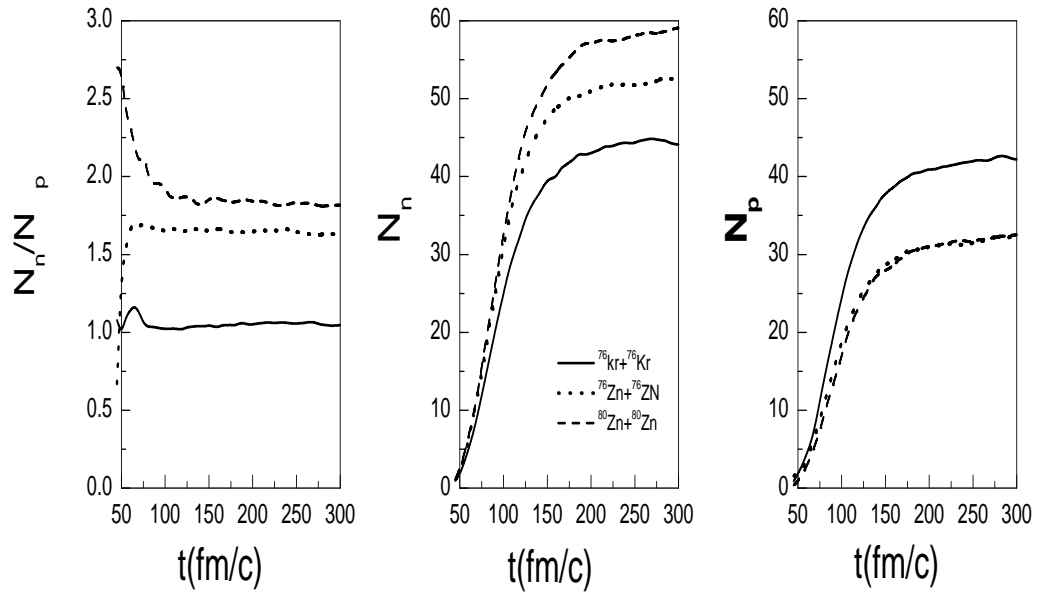


Figure 5: The time evolution of N_n/N_p (left window), N_n (middle window), and N_p (right window) for the systems $^{80}\text{Zn}+^{80}\text{Zn}$ (dash line), $^{76}\text{Zn}+^{76}\text{Zn}$ (dot line), and $^{76}\text{Kr}+^{76}\text{Kr}$ (solid line) at $E=100\text{MeV/u}$, $b=1.0\text{fm}$, and in the case of $U^{sym} + \sigma^{iso}$

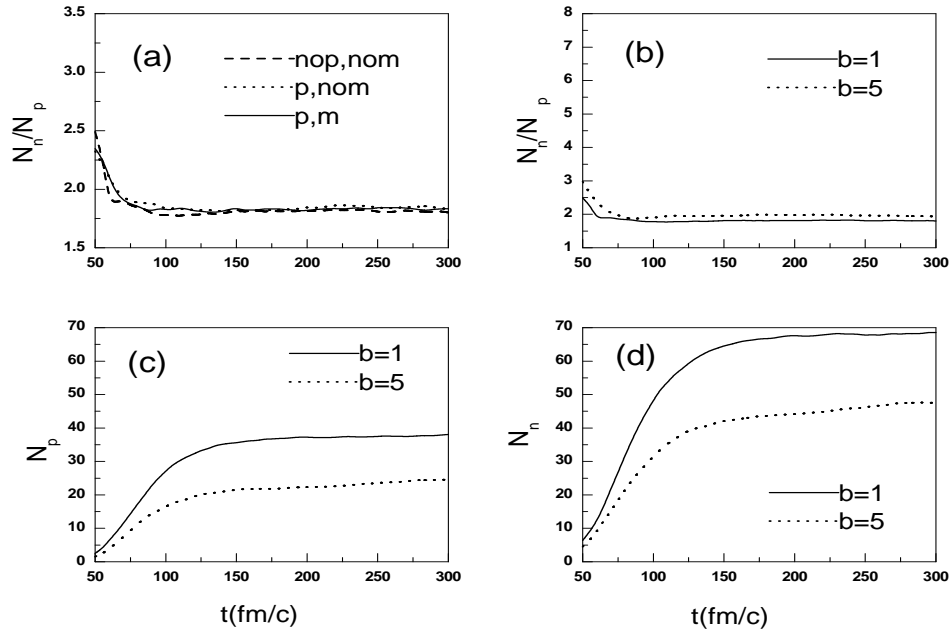


Figure 6: The time evolutions of $\frac{N_n}{N_p}$ (a) for the system $^{80}\text{Zn} + ^{80}\text{Zn}$ at $E=150\text{MeV/u}$ and $b=1.0\text{fm}$ for the three cases: 1) indicating Pauli and momentum dependent potentials (solid line), 2) indicating only Pauli potential (dot line), 3) indicating none of them (dash line). The time evolutions of $\frac{N_n}{N_p}$ (b), N_n (c), and N_p (d) for the system $^{80}\text{Zn} + ^{80}\text{Zn}$ at $E=150\text{MeV/u}$, $b=1.0\text{fm}$ (solid line), and $b=5.0\text{fm}$ (dot line).

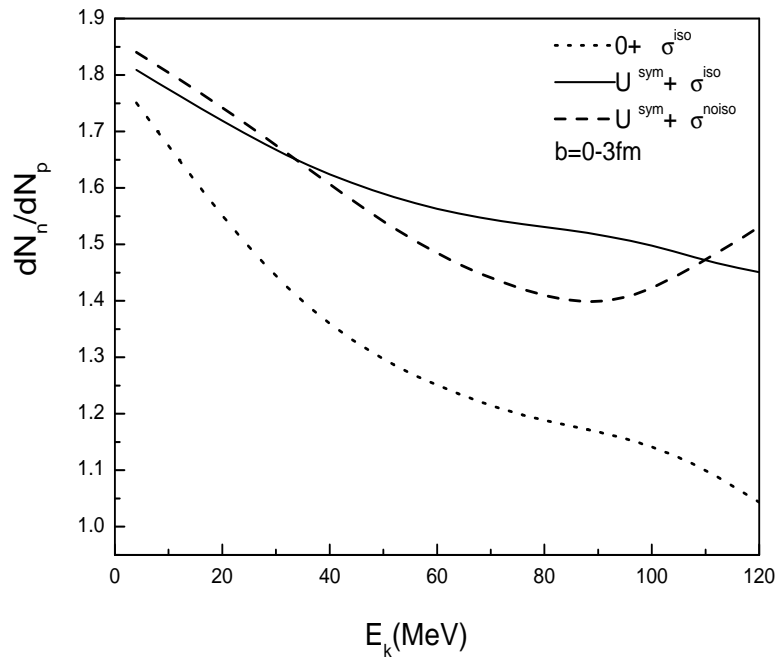


Figure 7: The impact parameter averaged kinetic energy spectra ($b=0.0, 1.0, 2.0, 3.0$ fm) of the preequilibrium emission ratio of neutrons to protons for the reaction $^{76}\text{Zn}+^{76}\text{Zn}$ at the beam energy $E=100$ MeV/u under three cases the same as Fig.3